Steel and Composite Structures, *Vol. 23, No. 5 (2017) 501-516*
DOI: https://doi.org/10.12989/scs.2017.23.5.501

Employing a fiber-based finite-length plastic hinge model for representing the cyclic and seismic behaviour of hollow steel columns

Mojtaba Farahi and Saeed Erfani *

Department of Civil Engineering, Amirkabir University of Technology, Tehran, Iran

(*Received September 28, 2016, Revised December 31, 2016, Accepted January 23, 2017*)

Abstract. Numerical simulations are prevalently used to evaluate the seismic behaviour of structures. The accuracy of the simulation results depends directly on the accuracy of the modelling techniques employed to simulate the behaviour of individual structural members. An empirical modelling technique is employed in this paper to simulate the behaviour of column members under cyclic and seismic loading. Despite the common modelling techniques, this technique is capable of simulating two important aspects of the cyclic and seismic behaviour of columns simultaneously. The proposed fiber-based modelling technique captures explicitly the interaction between the bending moment and the axial force in columns, and the cyclic deterioration of the hysteretic behaviour of these members is implicitly taken into account. The fiber-based model is calibrated based on the cyclic behaviour of square hollow steel sections. The behaviour of several column archetypes is investigated under a dual cyclic loading protocol to develop a benchmark database before the calibration procedure. The dual loading protocol used in this study consists of both axial and lateral loading cycles with varying amplitudes. After the calibration procedure, a regression analysis is conducted to derive an equation for predicting a varying calibrated modelling parameter. Finally, several nonlinear time-history analyses are conducted on a 6-story steel special moment frame in order to investigate how the results of numerical simulations can be affected by employing the intended modelling technique for columns instead of other common modelling techniques.

Keywords: cyclic behaviour; distributed plasticity finite element; fiber-based finite-length plastic hinge model; column members; cyclic strength deterioration; axial force-bending moment interaction

1. Introduction

Seismic assessment of existing buildings and the performance based design of new structures necessitate performing non-linear dynamic analyses (FEMA-P695 2009; PEER/ATC 2010). Reliable numerical models should be first provided for the intended structures before conducting the required nonlinear analyses. These numerical models should be capable of capturing the structural response of the intended structures from the elastic range through the global instability. In addition, computational efficiency is another concern during developing the mentioned nonlinear numerical models. Discrete Finite Element (DFE) modelling platforms such as OpenSees simulation platform have been commonly employed to conduct nonlinear time-history analyses. These simulation platforms are computationally more efficient than the platforms in which Continuum Finite Element (CFE) method is implemented. Hence, DFE simulation platforms are widely employed in earthquake engineering practice and research to simulate the seismic behaviour of different structures. The validity of these numerical simulations mainly depends on the accuracy of the modelling techniques that are utilized to simulate the seismic behaviour of the individual members of the intended structures.

Accordingly, numerous research studies have been carried out in order to develop robust and reliable modelling techniques for different structural elements. Variety of modelling techniques with different advantages and shortcomings has been developed by different researchers. As an instance, employing the concentrated plasticity models is one of the approaches that can be used to capture the nonlinear behaviour of structural elements (Giberson 1969). This approach can be simply applied and it helps to reduce dramatically the computational cost of simulations. As the most common instance, zero-length plastic hinges have commonly been implemented at the ends of beam members to simulate the nonlinear behaviour of these structural members (Ibarra 2005, Lignos and Krawinkler 2011, 2012). This approach is generally implemented to simulate the uniaxial nonlinear behaviour of an intended structural member. In addition, employing this approach demands for a constitutive law that should be first developed and calibrated based on available experimental data. However, comprehensive experimental databases have barely been developed for all types of structural members. As another alternative, fiber-based models can also be employed in order to simulate the nonlinear behaviour of structural members. In this modelling approach, the cross-section of structural members is discretized to nonlinear fiber elements (Hall and Challa 1995, Jin and El-Tawil

*Corresponding author, Assistant Professor,
E-mail: sderfani@aut.ac.ir

ISSN: 1229-9367 (Print), 1598-6233 (Online)

2003). Different nonlinear uniaxial material models with different hysteretic behaviour can then be assigned to the fiber elements. In this modelling technique, Distributed plasticity is captured through integration of a section response along the intended members. In addition, this modelling approach is capable of taking into account the interaction between the axial force and the bending moment contrary to the concentrated plasticity modelling approach. However, the computational cost of numerical simulations is increased if the distributed plasticity approach and fiber-based models are employed. This modelling approach has also been employed by different researchers in order to simulate the seismic behaviour of structural members (Uriz *et al*. 2008, Farahi and Mofid 2013, Salawdeh and Goggins 2013).

Steel hollow sections are used as columns of lateral load resisting frames in some countries with high seismicity such as Japan and Iran. Hence, in this study, it is intended to suggest and calibrate an appropriate modelling technique for hollow steel columns in order to overcome the shortcomings of common modelling techniques. It is worth noting that both aforementioned modelling approaches in previous paragraph have also been implemented in order to simulate the seismic behaviour of column members. As an instance, Lignos and Krawinkler (2012) employed the concentrated nonlinear hinges in order to simulate the nonlinear flexural behaviour of columns. They also tried to consider implicitly the deterioration of the seismic and cyclic behaviour of columns. Furthermore, Riberio et al. (Ribeiro *et al*. 2015) employed the same deterioration model to represent the moment-curvature behaviour in a different formulations. However, the axial force-bending moment (P-M) interaction in column members cannot be considered directly using this type of models. In other words, the axial behaviour of column members is suggested to be simulated independently where the mentioned concentrated plasticity models are used. On the other hand, Nam and Kasai modelled column members utilizing a fiber-based modelling approach (Nam and Kasai 2011). Moreover, a similar approach was implemented by Karamanci and Lignos (Karamanci and Lignos 2014) in *OpenSees* simulation platform. They divided the cross section of some wide flange columns into nonlinear fiber elements over a plastic hinge length. However, the deterioration of the cyclic behaviour of hollow steel columns cannot be taken into account directly if a fiber-based modelling approach is employed.

The model that has been utilized and calibrated in this study for simulating the behaviour of column members is a fiber-based modelling technique. Hence, this model is capable of accounting for the P-M interaction in column members. In order to overcome the general shortcoming of fiber-based models, the deterioration of the cyclic behaviour of columns due to local effects is considered implicitly in this study. Hence, a specific stress-strain constitutive relation is also calibrated in this study such that the cyclic deterioration can be captured by assigning this constitutive relation to the fiber elements representing the cross section of hollow steel columns. Consequently, the fiber-base Finite-Length Plastic Hinge (FLPH) model employed and calibrated in this paper have the advantages of both common modelling approaches discussed earlier, while its reliability is not undermined by the significant shortcomings of the mentioned modelling approaches. The calibration procedure for the fiber-based FLPH model is also performed based on a novel database of the cyclic behaviour of hollow steel columns developed in this study. This database is developed based on the cyclic behaviour of several column archetypes under a dual loading protocol consisting of both varying axial and lateral loading cycles (Farahi and Erfani 2016). To recapitulate, the study presented in this paper included three major steps:

- In the first step, a database of the cyclic behaviour of hollow steel columns is developed. This database is provided based on the behaviour of several column archetypes under a novel dual loading protocol.
- In the second step, a fiber-based FLPH model is introduced to simulate the behaviour of steel hollow sections using OpenSees simulation platform. This model is also calibrated based on the database developed in the first step.
- Eventually, the efficiency of the employed model is examined compared with other prevalent models as these models are implemented to simulate the seismic behaviour of the columns of a special moment frame.

2. Developing the benchmark database of the cyclic behaviour of hollow steel column members

An inclusive perception of the overall behaviour of hollow steel columns would be required at the early stage before developing and calibrating any modelling technique for these members. In addition, the calibration procedure for an intended model should be performed based on a database which reasonably represents the seismic and cyclic behaviour of these columns. Indubitably, high levels of axial and flexural demands are simultaneously developed in the columns of lateral load resisting frames during a severe ground motion. It is worth noting that both simultaneous structural demands on columns fluctuate dramatically during a seismic event. However, in almost all the previous experimental studies conducted on column specimens, lateral loading cycles in conjunction with a constant level of axial loading have been exerted on the intended specimens (Kumar and Usami 1996, Kurata *et al*. 2005, Newell and Uang 2008, Cheng *et al*. 2013). Consequently, it has been intended in this study to develop a novel database of the cyclic behaviour of hollow steel columns according to their behaviour under a more representative loading scenario. Thus, a database has been developed based on the response of several standard Hollow Structural Sections (HSS) archetypes under a dual loading protocol consists of both axial and lateral loading cycles with varying amplitudes (Farahi and Erfani 2016).

Experiments under simultaneous varying cycles of axial and lateral loading are almost rare in the literature. Performing such experiments under a dual loading protocol requires a complicated experimental set up. Thus, it has not

been planned in this study to explore the structural behaviour of the chosen column archetypes under a dual loading protocol through an experimental investigation. However, according to the previous experimental studies conducted under simpler loading pattern, it has been revealed that the cyclic behaviour of hollow steel column members is dominantly affected by the local geometric instabilities (Kurata *et al*. 2005, Nakashima and Liu 2005, Newell and Uang 2008). Based on the failure mechanism captured for the hollow steel columns in mentioned previous studies, it can be concluded that the behaviour of these structural members under cyclic loading scenarios can be accurately predicted by Continuum Finite Element (CFE) simulations. Accordingly, a CFE modelling framework has been used in this study to simulate the behaviour of different standard HSS archetypes under the intended dual loading protocol. The results of these CFE simulations were then utilized as the required benchmark for the next steps in this study. Before developing the intended database based on the results of CFE simulations, the accuracy of these simulations verified compared with available experimental results.

2.1 Continuum finite element framework used to develop the benchmark database

The CFE simulations were conducted using ABAQUS software in this study. Shell elements were chosen to model the HSS column archetypes because of the small thickness of these sections. Four-node reduced integration shell elements (S4R) with 6 degrees of freedom per node were employed among the available types of shell elements in the element library of ABAQUS. One end of the models provided for the column archetypes was fully constrained (at the bottom), while they were loaded at the other end. The edges of the free end of each numerical model were tied to a rigid plate, and the intended loads were exerted to a reference point at the middle of this rigid plate. During the previous experiments conducted on hollow steel column members under lateral cyclic loading (Kurata *et al*. 2005, Nakashima and Liu 2005), local geometric instabilities happened close to the fixed end of the specimens. Hence, the maximum mesh size at the upper 2/3 of the column archetypes was chosen to be two times of the maximum mesh size at the bottom 1/3 of them which is more prone to local buckling.

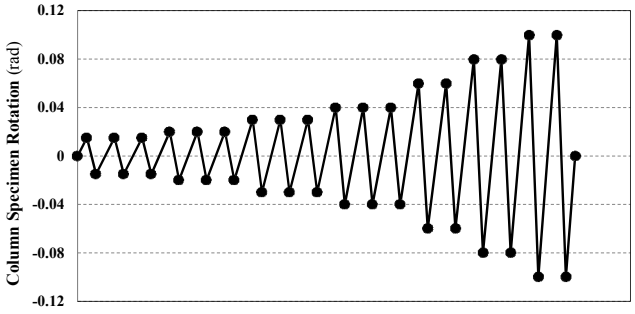

Fig. 1 Lateral loading cycles exerted on column specimens by Kurata *et al*. (2005)

Local imperfections are inevitably formed throughout structural elements due to fabrication and erection procedures. The effect of local imperfections on the overall behaviour of structural members cannot be neglected. This effect can be critical when structural members are subjected to high levels of axial loading and the local slenderness of these members is notable. In order to simply consider this effect, it was assumed that a linear combination of the first and the second buckling mode shapes of the column archetypes can represent the probable imperfect geometry of these members. The buckling mode shapes were obtained from an eigenvalue buckling analysis for each numerical model. Thus, the nodal displacements obtained from such an analysis as the first and the second mode shapes of each column archetype were scaled first. The scaled nodal displacements were then imported to the main numerical model provided for the column archetype as the probable initial imperfections.

The nonlinear behaviour of steel material was simulated through employing a combined hardening model because it has been proven that neither the kinematic hardening model, nor the isotropic hardening model can precisely simulate the general cyclic behaviour of steel material (Imani *et al*. 2015). Furthermore, in order to consider the effect of the probable contact between different faces of the column archetypes during the numerical simulations, the self-contact option of the software was also implemented in the CFE modelling procedure.

Numerical stability of the continuum finite element simulations was another concern. The implemented loading protocol included lateral cycles that called for large lateral deflections. Hence, large local plastic strains were expected to be evolved in parts of the column archetypes, which could risk the convergence of the simulations. ABAQUS finite element package involves a feature to mitigate such convergence problems by implementing damping throughout the model. The introduced viscous forces are sufficiently large to prevent instantaneous buckling or collapse, but small enough not to affect the overall behaviour while the solution is stable (ABAQUS 2012). In this study, the adaptive damping factor was used during the simulations changing from each increment to another increment. This factor is calculated such that the dissipated energy in each increment approaches a small fraction of the strain energy in the previous increment. This fraction is called the dissipated energy fraction and the default value equal to 0.05 set for this fraction in the CFE simulation.

2.1.1 Verifying the accuracy of the continuum finite element framework

The CFE framework explained in the previous paragraphs was utilized to capture available experimental results in the purpose that the accuracy of this numerical framework could be assessed. The experimental results reported by Kurata *et al*. (2005) were used in this study to verify the capability of CFE simulations in predicting the cyclic behaviour of steel hollow sections. The cyclic behaviour of six steel square hollow sections was investigated in these experiments (Kurata *et al*. 2005). The nominal size of all the specimens was 200 mm × 200 mm, while three different thicknesses were adapted to fabricate

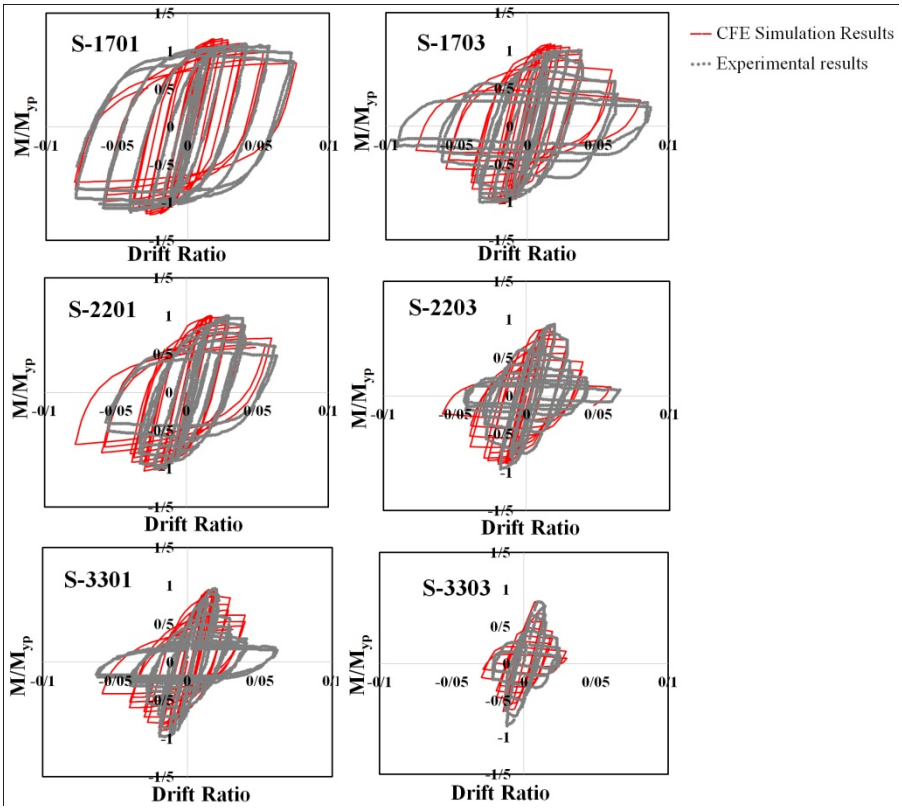

Fig. 2 End moment-rotation curves obtained from the experiments performed by Kurata *et al*. (2005) besides the curves obtained from the numerical simulations

specimens with 3 slenderness ratios (width-to-thickness ratio) equal to 33, 22 and 17. The material properties employed in FE models of the specimens tested by Kurata *et al*. were chosen based on what was reported by these researchers (Kurata *et al*. 2005). The loading scenario in these experiments included cycles of lateral displacements and a constant axial compressive force. The lateral loading cycles used by Kurata *et al*. are shown in Fig. 1. Each column specimen was tested under two constant levels of axial loading equal to 10% and 30% of the nominal axial capacity of that specimen. The experimental specimens were referred according to their slenderness ratio and the constant level of axial force during the relevant experiment. As an instance, S-2203 refers to the specimen with a slenderness ratio equal to 22 which was tested in the presence of a constant axial load equal to 30% of the nominal axial capacity of this specimen.

The results of these experiments were chosen for verifying the validity of CFE simulation results due to the fact that the range of the lateral loading cycles employed in them was close to the range of the lateral sequences in the dual loading protocol implemented in this study. The highest level of axial force in these experiments was also similar to the amplitude of the ultimate axial loading cycles of the intended protocol. Furthermore, the dimensions of the mentioned experimental specimens were not too different from the practical dimensions for structural columns.

The results of the mentioned experiments and the results obtained from the numerical simulations in this study have been depicted in Fig. 2. This figure shows the bending moment at the end of the specimens versus the imposed lateral drift. The bending moment has been scaled to the ultimate plastic flexural capacity of the specimens. As it can be inferred from this figure, the results of the CFE simulations match experimental results with a reasonable accuracy. The deformed shape of one of the specimens at the end of the experiment has also been compared with the deformed shape obtained from the numerical simulation in Fig. 3. The consistency between the deformations happened during the experiments and the deformations predicted by the CFE simulations prove the ability of the employed CFE framework in capturing the correct failure mechanism. Based on the Figs. 2 and 3, it can be concluded that the cyclic behaviour of hollow steel columns can be numerically simulated with an acceptable accuracy using the CFE modelling framework discussed in this part. Hence, this CFE modelling framework can be employed in order to develop a reliable database of the cyclic behaviour of hollow steel columns in the next part of this study.

The experimental results reported by Kurata *et al*. (2005) were also used to finalize some CFE modelling details before performing the final simulations. Several trial simulations were performed to find the appropriate scaling factors for the imported nodal displacement from the eigenvalue analyses. These scaled nodal displacements were imported to the main numerical model of each specimen to represent the initial imperfections. Eventually, the nodal displacements regarding to the first and the second buckling mode shapes of each specimen were scaled up with the factors equal to 1.5 and 1 respectively before

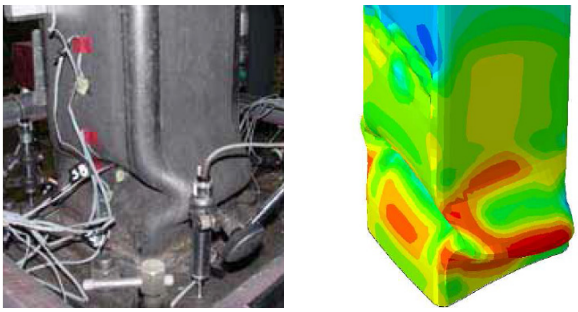

(a) (b)

Fig. 3 (a) Deformed shape of specimen S2203 at the end of the experiment (2005); (b) deformed shape of specimen S2203 predicted by the CFE simulation performed in this study

being imported in the main numerical models to get the best match with the experimental results. In addition, performing the simulations with the minimum mesh size less than 20mm did not result in perceptibly different moment-rotation curves. Hence, the smallest mesh size was chosen finally equal to 20 mm in this study.

2.2 Simulating the cyclic behaviour of column archetypes with hollow sections

The required database in this study has been developed by simulating the cyclic behaviour of numbers of column archetypes. First, the column archetypes were chosen from standard square HSS sections in this study. In order to limit the number of column archetypes, only the HSSs with compact cross-section geometry were chosen as the column archetypes. According to table D1.1of AISC 341-10 (AISC 2010), the width-to-thickness ratio should not exceed $1.12\sqrt{\frac{E}{F_y}}$ for the webs of columns with square hollow sections which are intended to be utilized in seismic prone regions. In addition, only the square HSSs fabricated from ASTM A500 Grade C and Grade D steel material were selected. The yield stress of these types of steel material is equal to 345 MPa (50 ksi) and 248 MPa (36 ksi) respectively. In addition, a strain hardening ratio equal to 0.5% was assumed for steel material in this study. Based on the above limitations, the sections listed in Table 1 were finally selected as the sections of the column archetypes. The length of all the column archetypes was chosen equal to 3200 mm. The geometric properties of the chosen archetypes have been also included in Table 1.

Columns are subjected to simultaneous axial and bending moment during earthquakes. In addition, both of these structural demands on columns fluctuate during a seismic event. In this research, it was decided to employ a loading protocol which represents the realistic range of both mentioned seismic demands on columns and their rate of fluctuations. Hence, a dual loading protocol that has recently been developed by the authors (Farahi and Erfani 2016) was used in this study to load the column archetypes. This loading protocol represents the simultaneous flexural and axial demands on the column members of steel Special Moment Frames (SMF) that might developed in these members during a seismic event with the Maximum Considered Earthquake (MCE) seismic intensity level (Farahi and Erfani 2016). This loading framework consists of a series of drift ratio cycles in conjunction with a series of axial load ratio cycles. The drift ratio is defined as the ratio of the relative lateral displacement of a column to its length and the axial force ratio refers to the ratio of the imposed axial load to the nominal axial yield capacity of a column. The lateral and axial loading cycles of the dual loading protocol have been summarized in Tables 2 and 3.

Table 1 Geometric properties of the chosen archetype columns

Standard hollow section	Nominal width (cm)	Thickness (mm)	Width to thickness ratio	Cross-section area (cm^2)	Plastic module (cm^3)
HSS 12×12×5/8	30.5	15.9	17.7	165.8	1786.2
HSS 14×14×5/8	35.6	15.9	21.1	195.5	2474.4
HSS 16×16×5/8	40.6	15.9	24.5	225.8	3277.4
HSS 18×18×5/8	45.7	15.9	25.8	267.1	4326.2
HSS 20×20×5/8	50.8	15.9	29	299.4	5424.1

Table 2 Lateral loading cycles of the employed dual loading protocol (Farahi and Erfani 2016)

Drift ratio peak	Number of cycles
0.002	12
0.003	12
0.006	10
0.0075	10
0.0125	6
0.02	6
0.03	2
0.04	1
0.06	1

Table 3 Axial loading cycles of the employed dual loading protocol (Farahi and Erfani 2016)

Axial force ratio peak	Number of cycles
-0.175	12
-0.2	12
-0.225	12
-0.25	10
-0.35	6
-0.4	4
-0.425	4

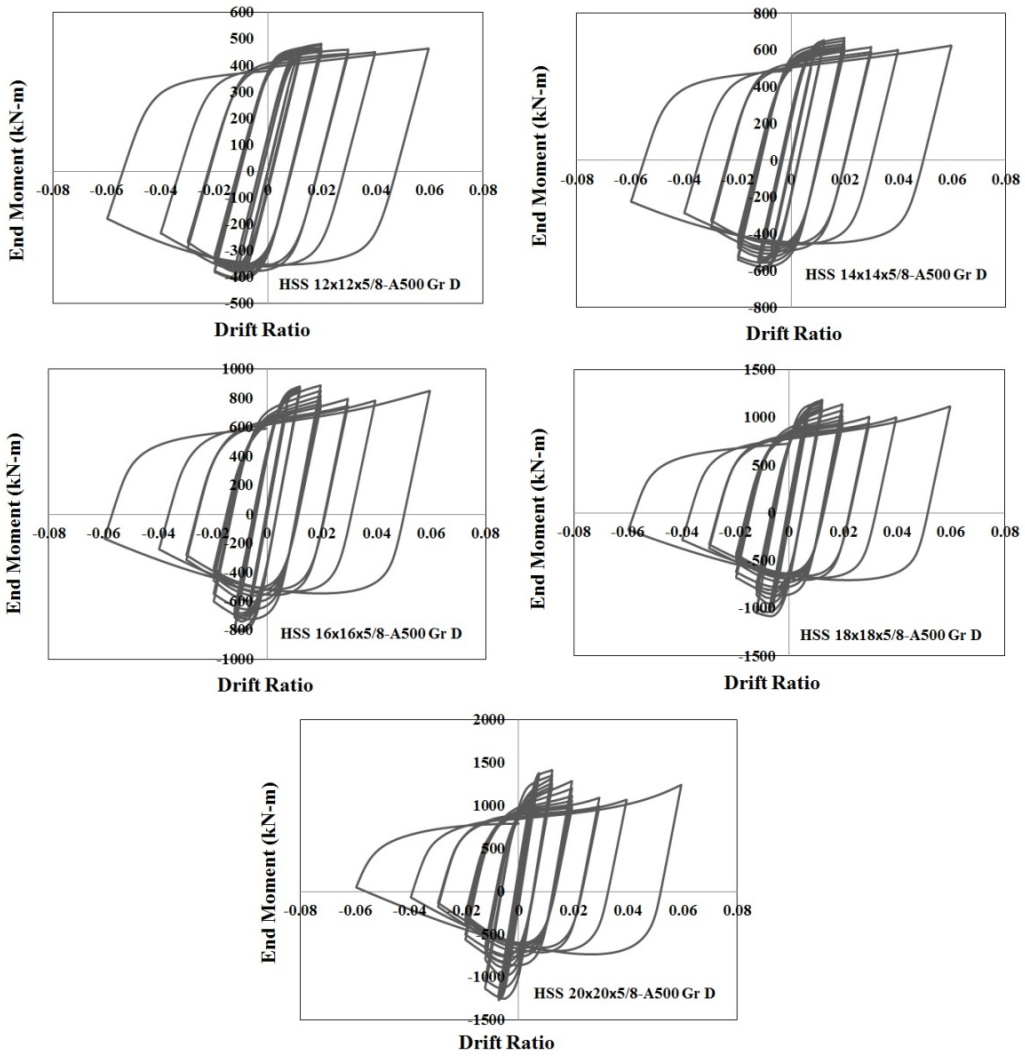

Fig. 4 End bending moment-nominal rotation curves for the column archetypes built up from ASTM A500 grade D steel material

After the column archetypes and the loading scenario were chosen, the nonlinear behaviour of the HSS column archetypes under the selected dual loading protocol was simulated using the continuum finite element framework introduced in the previous part. Axial and lateral loading cycles introduced in Tables 2 and 3 were exerted on the column archetypes simultaneously and in the same analysis step during the simulations.

Fig. 4 shows the end bending moment-nominal rotation curves for all the column archetypes built up from ASTM A500 grade D steel material. Nominal rotation refers to the ratio of the lateral displacement at the free end of each column archetype to its length. The similar curves have been shown in Fig. 5 for the archetypes fabricated from ASTM A500 grade C steel material.

As it is evident from Figs. 4 and 5, the rate of deterioration in the cyclic behaviour of the column archetypes intensifies as the slenderness of their sections increases. This fact proves the dominant effect of local buckling on the seismic and cyclic behaviour of steel columns. In addition, comparing Fig. 4 with Fig. 5 reveals that the deterioration rate decreases slightly with increasing the material strength. The experimental data gathered and reported by Lignios and Krawinkler (2012) also proves the same relations between the deterioration rate in the cyclic behaviour of columns and their local slenderness and material properties. Eventually, the results of the CFE simulations have been considered as a benchmark that represents the general cyclic behaviour of hollow steel columns with the width to thickness ratio ranges from 17 to 30.

3. Introducing a fiber-based FLPH modelling technique for column members

As the main aim of this study, a fiber-based FLPH modelling technique was calibrated and employed in order to simulate the seismic and cyclic behaviour of column members. This modelling technique was employed with the aid of modelling features of Opensees simulation platform (OpenSees 2015). Among different types of modelling approaches, a fiber-based approach was employed in this research. Hence, the cyclic behaviour of several HSS columns obtained in the previous step has been utilized as a

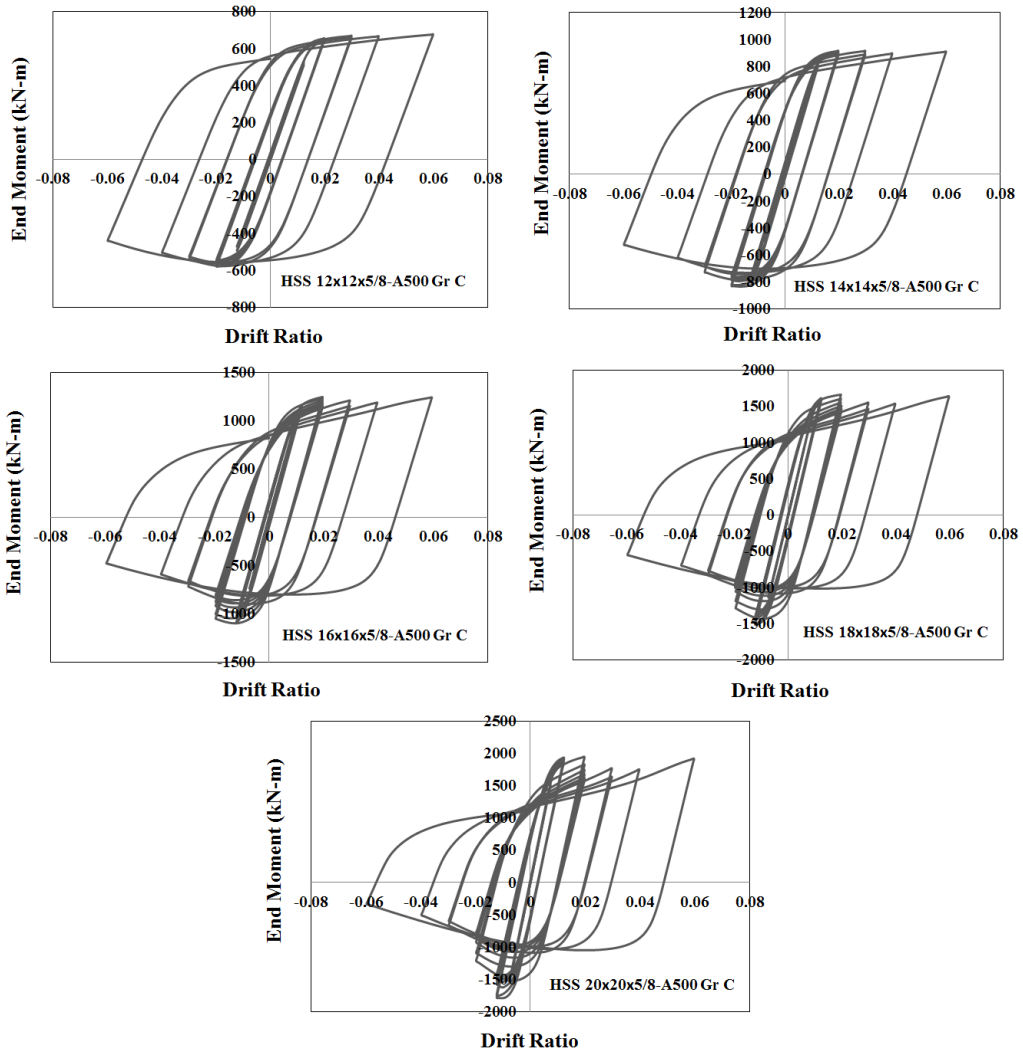

Fig. 5 End bending moment-nominal rotation curves for the column archetypes built up from ASTM A500 grade C steel material

benchmark database to calibrate the material model assigned to the fibers in the suggested fiber-based modelling technique. Since the cross-section of columns is discretized to nonlinear fibers in the intended modelling technique, the simulation results are dominated by the nonlinear behaviour of the material model assigned to the fibers. As a merit of the fiber-based FLPH modelling technique, the interaction between the bending moment and the axial force in any intended column member is considered directly. In addition, the distributed nonlinear behaviour can be captured along a specified length of the member. Contrary to prevalent fiber-based models, the intended model also accounts for the deterioration of the cyclic behaviour of columns (Hamidia *et al*. 2014, Dimopoulos *et al*. 2016, Tzimas *et al*. 2016).

The cyclic deterioration of the behaviour of hollow steel columns should necessarily be considered as it is aimed to simulate the cyclic behaviour of these members. Hence, considering the cyclic deterioration effect was one of the main concerns in this research as the fiber-based approach was chosen to develop the intended modelling technique. In order to implicitly consider the probable deterioration in the hysteretic behaviour of column members, a certain nonlinear material model that is known as Bilin Material was assigned to the fibres across the section of any intended column. The initial stiffness and the ultimate strength capacity of this material model can be deteriorated during the simulation. The rate of this deterioration is controlled by the rule proposed by Ibarra *et al*. (2005). Based on the mentioned rule, a reference hysteretic energy dissipation capacity, E_t, is assumed for each intended structural member. This capacity is an inherent property of each member which is not affected by the loading history applied to the member. The reference hysteretic energy dissipation capacity is defined as a multiple of the yielding energy which is obtained by multiplying the yielding strength to the yielding deflection of each intended member. Consequently, E_t can be considered as a multiplier of the yielding strength. The multiplier in this rule, Λ, is called deterioration parameter and it can be assessed by users as a modelling parameter during introducing the material model to the software. The rate of the strength and stiffness deterioration in each exertion is determined based on the rate of the energy dissipated in the previous exertion

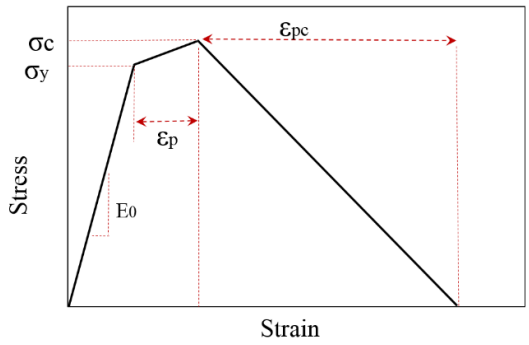

Fig. 6 Required modelling parameters to define the stress bounds of the material model used in this study

compared to the reference hysteretic energy dissipation capacity assumed for the intended member. Hence, selecting a larger value for the deterioration parameter results in a lower cyclic strength and stiffness deterioration rate under a cyclic loading. However, this material model was first simplified before it was calibrated in this study. Fig. 6 shows the required parameters to define the simplified version of the mentioned material model (except the deterioration parameter) in terms of stress and strain. Other modelling parameters of the original version of Bilin Material model were excluded from the version employed in this study. The benchmark data base of the cyclic behaviour of hollow steel columns provided in this study did not necessitate considering a residual strength for fibers. Maybe this is because of the fact that amplitude of the lateral loading cycles used in this study was limited to a drift ratio equal to 0.06 rad. Hence, the authors preferred to remove this modelling parameter for the sake of simplicity. E_0, a_{sh}, and σ_y represent the initial stiffness, strain hardening ratio and the yielding strength respectively. The strength back-bone of this material can be defined by specifying appropriate values for ε_p (pre-capping plastic strain) and ε_{pc} (post-capping plastic strain) in addition to the aforementioned parameters.

In the intended modelling technique, each column member is divided into two parts with the same length that are offset in the mid-length of the member. This initial chamber triggers the global flexural buckling in the intended column members and it was chosen equal to 0.1% of the length of each column.

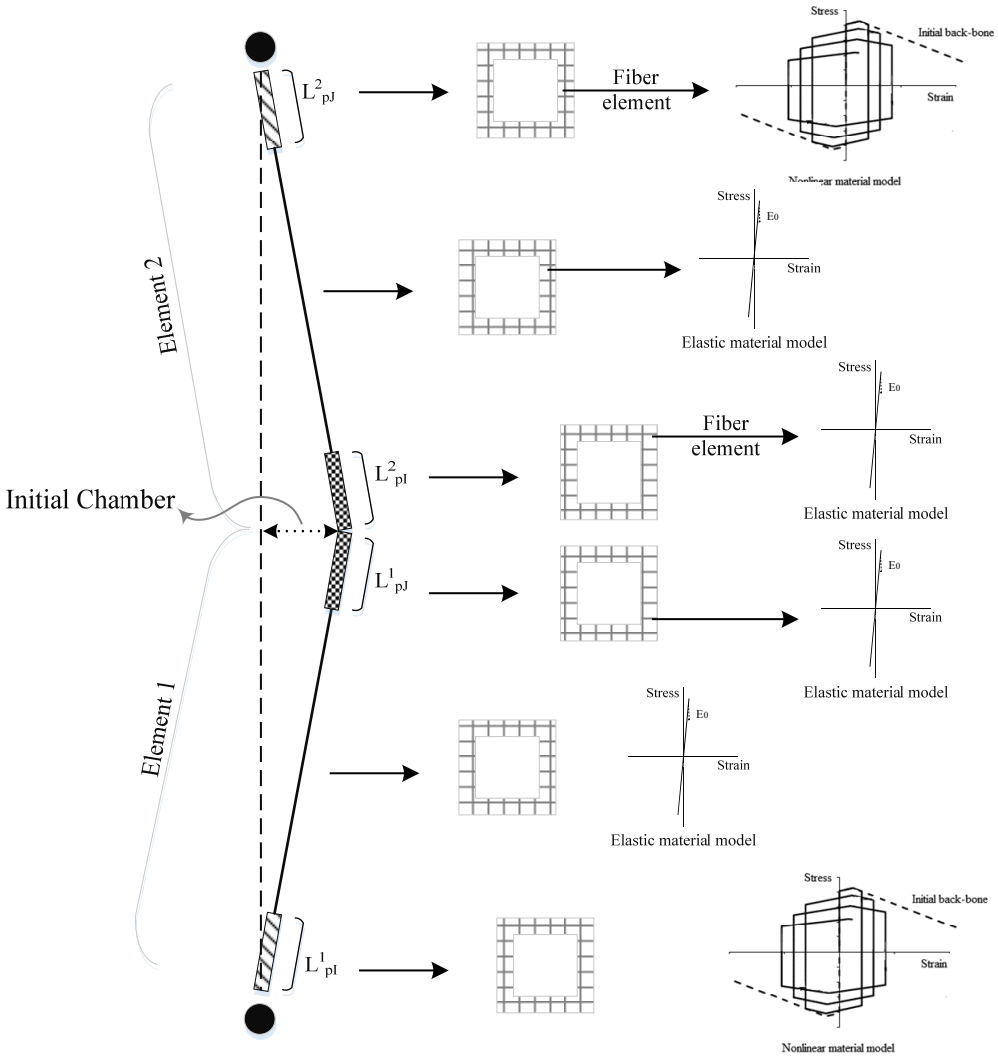

Fig. 7 Schematic description of the modelling technique developed in this study for steel columns

A fiber-based approach (distributed plasticity) can be employed in Opensees simulation platform by using the force-based beam-column elements. The cross section of these elements can be then discretized to nonlinear fibers along their entire length. However, localization issue can be raised in this case because of the softening part in the material model assigned to fiber elements (Coleman and Spacone 2001). In addition, time-history analyses would be very time-consuming in that case. Hence, In order to evade the mentioned problems, the plastic behaviour was limited to discrete regions (plastic hinges) at the ends of the intended column members, and the regularized hinge integration method (using Radau intergration approach) (Scott and Hamutçuoğlu 2008, Scott 2011) was employed in the suggested modelling technique. In case of utilizing this integration method, two different section can be assigned to the plastic regions at both ends of an element. In addition, the plastic hinge length at both ends of a member, lpI and lpJ respectively, can be specified separately. The nonlinear behaviour of each plastic hinge is determined through defining the nonlinear sections with tags secTagI and secTagJ. These nonlinear sections, secTagI and secTagJ, are then assigned to the plastic regions at the beginning and at the end of any intended element respectively. As mentioned before, the required nonlinear sections were defined by discretizing the cross-section of column members to nonlinear fiber elements in plastic regions. The behaviour of the remained length of columns between the plastic hinges was assumed to be linear. As stated before, it was decided to use two elements to model each column member in order to create the initial chamber. Hence, nonlinear fiber-based sections were assigned only to the beginning region of the first element and the end region of the second element as it has been depicted in Fig. 7.

3.1 Calibrating the fiber-based FLPH modelling technique based on the cyclic behaviour of the column archetypes

The fiber-based FLPH model has been employed in this part to simulate the cyclic behaviour of the HSS column archetypes (part 2.2) using OpenSees simulation platform. That is, it was tried to employ the database of the cyclic behaviour of hollow steel columns provided in part 2.2 in order to calibrate the developed fiber-based FLPH modelling technique. As it is apparent from Figs. 4 and 5, the strength of the column archetypes was notably deteriorated under the cyclic loading. The rate of this deterioration was not the same for different archetypes with different width to thickness ratios and different constituent materials. Hence, for each HSS column model, an appropriate unique deterioration parameter should be chosen for the material model assigned to the fibers in the plastic hinges. Furthermore, the stress bounds and the back-

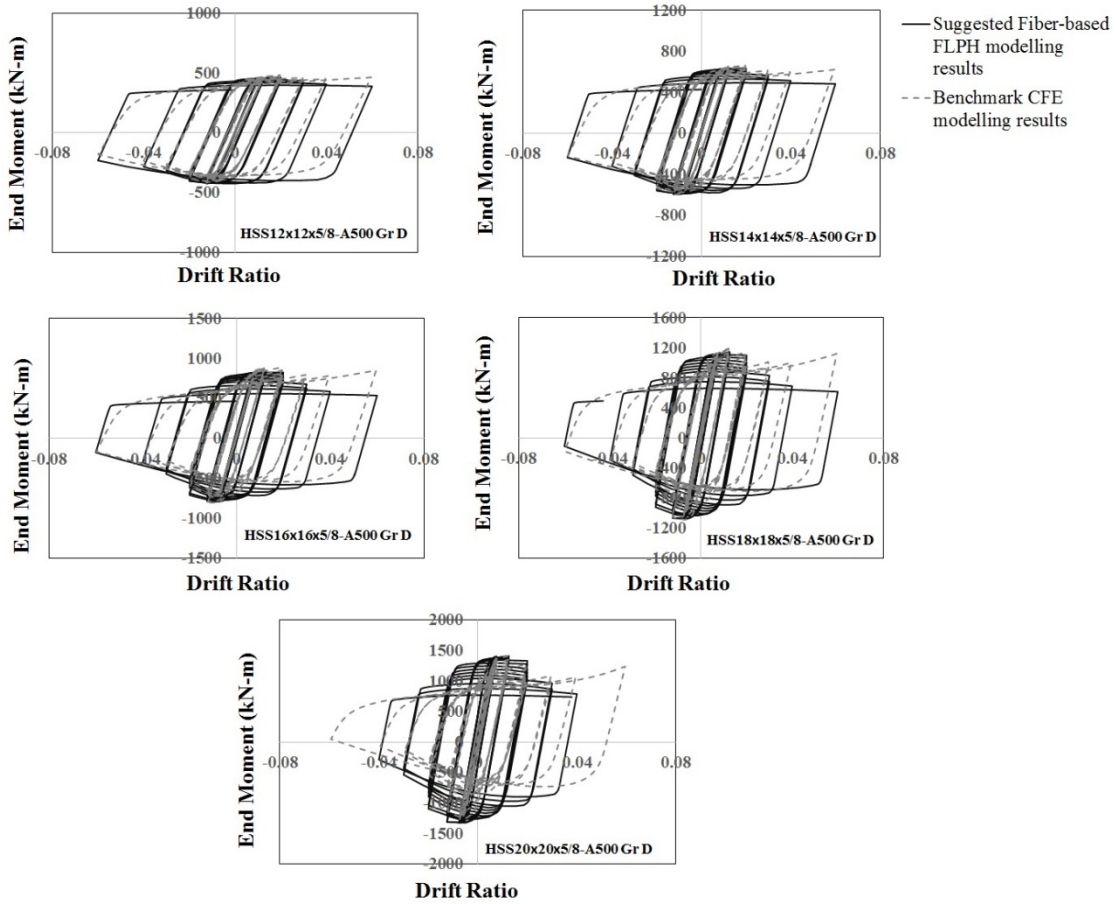

Fig. 8 Results obtained by implementing the fiber-based FLPH modelling technique for column archetypes built up from steel of type A500 grade D

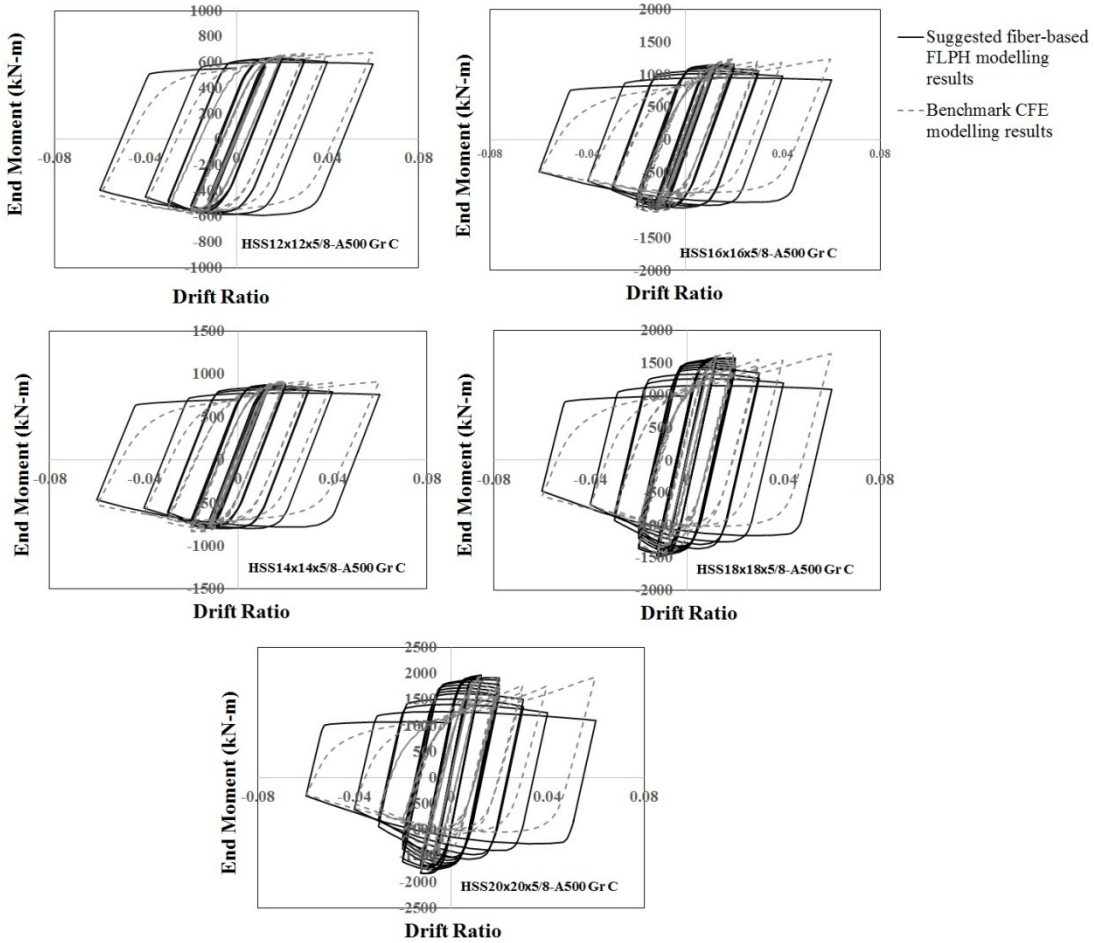

Fig. 9 Results obtained by implementing the fiber-based FLPH modelling technique for column archetypes built up from steel of type A500 grade C

bone of the material model employed in the plastic regions should be determined by choosing appropriate values for ε_p and ε_{pc}.

An elastic fiber-based section has been chosen to represent the cross section of the remained part of the column archetypes between the fiber-based finite length plastic hinges. The same discretization plan was employed for the linear and the nonlinear sections. Ten and three fiber elements were employed along the length and through the thickness of the cross sections of the column archetypes. Several initial simulations were performed to investigate the effect of the number of fibers on the predicted results. However, employing more fibers barely affected the simulation results, while it increased the time of the simulation.

The elastic material assigned to the fiber elements of the elastic sections was simply defined employing the elastic modulus of the relevant steel material. However, the mentioned modelling parameters should be evaluated first in order to define the uniaxial stress-strain constitutive relation assigned to the fiber elements of the inelastic sections. Hence, a calibration study was conducted in order to choose the appropriate values for the modelling parameters required for defining the material model implemented in this study. Before the calibration study, the suitable values for σ_y and E_0 were chosen based on the properties of the steel materials of types ASTM A500 grade D and grade C. Furthermore, preliminary trial simulations to capture the cyclic behaviour of HSS columns in the provided database proved that the appropriate values for other parameters required for defining the back-bone of the material model (a_{sh}, ε_p and ε_{pc}) are not significantly influenced by the geometry of the archetypes. It was also demonstrated by these trial and error analyses that a_{sh}, ε_p and ε_{pc} can be set equal to 0.005, 0.015 and 0.25 respectively when the behaviour of the column members built up from steel of type A500 grade D is modelled. In case of modelling of the steel columns fabricated from the steel material of type A500 grade C, the mentioned parameters can be set equal to 0.005, 0.015 and 0.35 respectively. However, different deterioration parameters had to be adapted for different cases in order to fit the new simulation results (obtained by employing the fiber-based FLPH technique) to the benchmark database developed previously. Several trial simulations were performed to find the most appropriate deterioration parameter for simulating the cyclic behaviour of each column archetype. Figs. 8 and 9 show the results obtained when the calibration procedure of the fiber-based FLPH technique was finalized. The end moment-nominal rotation curves from the benchmark database obtained in part 2.2 have been also depicted in these figures.

In fiber-based formulation, it is assumed that sections remain plain. However, large plastic deformations can induce severe local buckling. It should be noted that the rate cyclic deterioration in the behaviour of sections in conjunction with the capping and post capping capacity of the material assigned to the fibers have been calibrated in the model used in this study in order to consider implicitly the effects of such local instabilities that belie the initial assumption.

As mentioned, different values should be assigned to the deterioration parameter to capture the cyclic behaviour of different columns with different width to thickness ratios and material properties. Hence, the appropriate value for the deterioration parameter can be assessed as a function of the mentioned variables. In order to develop such a function based on the results of this study, a stepwise multivariate regression analysis (Chatterjee *et al*. 2000) was also conducted. The function was chosen to be in the form represented by Eq. (1) because it has been found by other researchers that a general predictive power law-fitting model has been a reasonable choice in similar cases (Lignos and Krawinkler 2012, Hsiao *et al*. 2013, Karamanci and Lignos 2014).

$$\Lambda = a_1.(PV_1)^{a_2}.(PV_2)^{a_3}...(PV_n)^{a_{n+1}}.\varepsilon \quad (1)$$

In this equation, a_i is the constants that are calculated from the multivariate regression analysis for each intended predictive variable PV_i, and ε is the random error. The predictive variables in this study were chosen based on the geometric and material properties that were varied among the archetype columns. The first PV was selected as the ratio of the width of column members (d) to the thickness of these members (t), and $\left(\frac{E}{F_y}\right)$ was selected as the second PV. E and F_y represent the Young's modulus and yield stress of the intended steel columns, respectively. Lignos and Krawinkler (2012) employed standard t-test and F-test to prove the significance of the mentioned predictive variables for predicting the cyclic deterioration in the behaviour hollow steel columns using a database of the available experimental results. By transferring the data to logarithmic domain, Eq. (1) can be rewritten in the form of Eq. (2).

$$\begin{aligned}\log(\Lambda) &= \log(a_1) + a_2\log(PV_1) + a_3\log(PV_2) \\ &....+ a_{n+1}\log(PV_n) + \varepsilon\end{aligned} \quad (2)$$

Eventually, the multivariate linear regression analysis was carried out to evaluate the constants. Eq. (3) is the finalized function for predicting the deterioration parameter that was obtained based on the regression analysis.

$$\Lambda = 413.143 \cdot \left(\frac{d}{t}\right)^{-1.367} \cdot \left(\frac{E}{F_y}\right)^{-0.195} \quad (3)$$

Fig. 10 shows the values of Λ predicted by the developed equation versus the values obtained for this parameter during the calibration procedure for the column archetypes (circular shaped dots). This figure shows a good match between the values calculated using Eq. (3) and the results of the calibration procedure. Since the loading and the boundary condition were the same for all the HSS archetypes during developing the benchmark database, the data provided in Fig. 10 is not scattered. Moreover, the coefficient of determination, R^2, was calculated equal to 0.938 which suggests that the developed equation explains approximately 94% of the variability in the response variable Λ.In addition, the vector of residuals ranged between -0.0392 to 0.0523 for the observations, and the error variance was estimated equal to 0.0011.

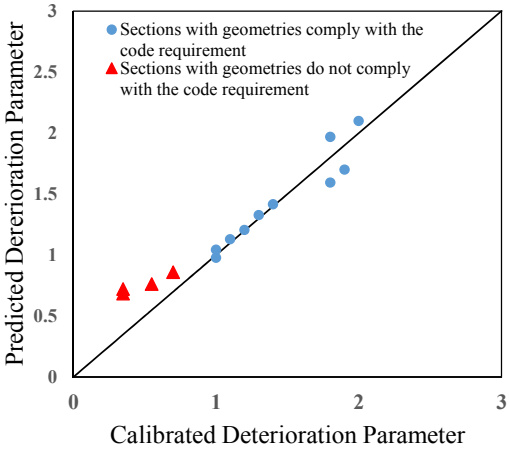

Fig. 10 Values obtained for the deterioration parameter from Eq. (3) versus the values derived from the calibration procedure for the HSS archetypes

It is worth noting that, the regression analysis was only performed based on the limited benchmark database developed in this study. However, the geometry and width to thickness ratio of the web of any other built up box-shaped sections that comply with the provisions of AISC 341-10 (AISC 2010a) cannot be beyond the range of width to thickness ratios we considered in this study. Hence, the developed formulation is expected to be valid for all the hollow box-shaped sections that can be used practically as structural columns in seismic prone regions.

In addition, the same calibration procedure has also been conducted for some square HSS columns with the width to thickness ratios greater than $1.12\frac{E}{F_y}$ (HSS 20 × 20 × 1/2, HSS 22 × 22 × 5/8, HSS 24 × 24 × 5/8, HSS 26 × 26 × 5/8). The results have been depicted in Fig. 10 with triangular-shape dots. As it can be expected, the results of the calibration procedure for the mentioned sections with highly slender webs generally deviated from the values obtained from Eq. (3). Hence, the deterioration rate of the cyclic behaviour of hollow sections increases significantly for the hollow sections with the width to thickness ratios greater than $1.12\frac{E}{F_y}$.

It is expected that more experiments would be conducted on column members under the loading scenarios that are consistent with the range of real seismic demands

on these members. Future experiments may reveal more details about the magnitude and the fluctuation rate of both axial and bending demands on column members. Hence, the results of such experiments can definitely be employed then to improve the database developed in this study. Meanwhile, the fiber-based FLPH modelling technique calibrated in this study can be implemented for predicting the seismic and cyclic behaviour of square HSS column members fabricated from standard steel of types ASTM A500 grades C and D with the width to thickness ratios range between 17 and 30.

4. Effect of using the fiber-based FLPH modelling technique on the results of the numerical simulations conducted on a steel frame archetype

In the final stage of this research, it has been tried to decipher how the results of numerical simulations (conducted with the aid of OpenSees) can be affected if the developed modelling technique is used to model the column members of special moment frames (SMF). Hence, the seismic behaviour of a steel special moment frame (SMF) archetype was numerically investigated in this part. In order to provide the required nonlinear model of the chosen frame archetype, the modelling technique calibrated in this study as well as two other types of prevalent modelling techniques were employed to simulate the nonlinear behaviour of the column members of the selected SMF. The SMF archetype was assumed to be one of the lateral load resisting frames of a 6-story building with the plan shown in Fig. 11. The building was first loaded and designed according to ASCE/SEI 7-10 (2010) (ASCE) (ASCE) (ASCE) and AISC 360-10 (AISC 2010b) respectively. The

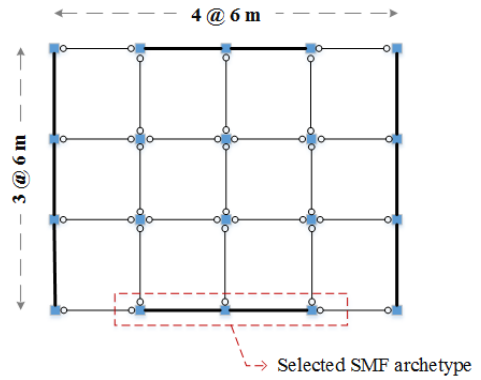

Fig. 11 Plan view of the sample 6-story building

Table 4 Summary of the designed sections for the SMF archetype

Story	Column section	Beam section
1,2	HSS 18×18×5/8	W16×100
3,4	HSS 18×18×5/8	W16×89
5	HSS 16×16×5/8	W14×61
6	HSS 16×16×5/8	W14×30

seismic provisions of AISC 340-10 (AISC 2010a) were also taken into account designing the lateral load resisting system (SMFs) of the building. The results of the design procedure have been summarized in Table 4. The height of all the stories of the building was chosen the same and equal to 3.5 m except the height of the first story which was considered equal to 4 m. The distributed dead load on the floors was assumed to be equal to 4.0 kN/m^2. The values of 2.0 and 1.5 kN/m^2 were considered as the live loads on the floors and on the roof of the building, respectively. As it is apparent from Table 4, wide flange sections were assigned to the beam members, and the sections of the columns were chosen from HSSs.

4.1 Providing numerical models for the selected SMF

In order to conduct nonlinear analyses, three different nonlinear models were developed in OpenSees simulation platform for the 6-story 2-span special moment frame archetype. The nonlinear behaviour of beams in the three models was taken into account using end zero-length plastic hinges. Zero length elements were used to model the plastic hinges, and elastic beam-column elements were employed to model beam members between the end hinges. Bilin material model from the OpenSees uniaxial material library was assigned to the section of the zero-length elements at the ends of the beams. The required parameters to define Billin material model were evaluated based on the formulations suggested by Lignos and Krawinkler (Lignos and Krawinkler 2011, 2012).

However, the columns of the SMF archetype were modelled using three different techniques including the developed modelling technique for columns in this study. Hence, the only difference between these three models was the modelling technique used to simulate the seismic behaviour of the columns. The details of the modelling technique calibrated in this paper were explained in previous parts. The numerical model provided using this modelling technique has been referred in this study as Model1-FB-FLPH. In the second model which has been named Model2-FB, a distributed plasticity technique was utilized to simulate the nonlinear behaviour of the column members. In this model, the cross section of the columns was discretized to the nonlinear fiber elements along their entire length. A material model known as Steel02 in the uniaxial material library of OpenSees was assigned to the fiber elements. This uniaxial bilinear material model has been developed by Menegotto and Pinto (Menegotto and Pinto 1973). In order to define the overall back-bone of this material in OpenSees simulation platform, the material yield stress, Fy, the elastic modulus, E, and the strain-hardening ratio, b, should first be specified. F_y and E were evaluated based on the standard material properties of steel type ASTM A500 grade D, and the strain-hardening ratio (ratio of post-yield tangent to initial elastic tangent) was assumed equal to 0.02. In order to develop the third model of the SMF archetype, the concentrated plasticity approach was used to simulate the nonlinear behaviour of the column members. This approach is exactly the same as the modelling approach implemented to simulate the nonlinear

behaviour of beam members in this part. Bilin uniaxial material was employed to define the nonlinear behaviour of zero-length hinges at the ends of columns. Lignos and Krawinkler (2012) also calibrated this material model to represent the cyclic behaviour of column members. Hence, They suggested different formulations for the required modelling parameters of this uniaxial material when it is intended to be used for modelling the behaviour of column members (Lignos and Krawinkler 2012). These formulations relate the required modelling parameters not only to the geometric and material properties of the intended cross sections, but also to the level of axial force in column members. The average axial force in the column members was assumed to be equal to 20% of their yield axial capacity in order to calculate the required modelling parameters in this research. The last model has been named Model3-ZLPH in this study.

4.2 Time-history analyses

The seismic response of the three models developed in this part (for the selected SMF) has numerically been simulated under several ground motion records. The records used in this study have been chosen randomly from the far-field record set suggested by FEMA P695 (2009). These records have been introduced in Table 5, and an ID number has been assigned to each record in this table. The time-history analyses were then performed under each of the selected seismic records with different intensities (incremental dynamic analyses). The intensity of the base excitations were determined by the scale factors multiplied to each seismic record before conducting the simulations.

Table 5 Ground motion records used in this study

Record ID	Earthquake name	Magnitude	Year
1	Northridge	6.7	1994
2	Imperial Valley	6.5	1979
3	Imperial Valley	6.5	1979
4	Kocaeli, Turkey	7.5	1999
5	Manjil, Iran	7.4	1990

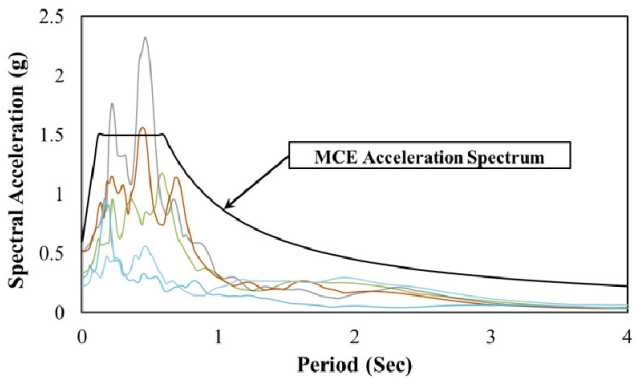

Fig. 12 Acceleration response spectra of the implemented seismic records in conjunction with MCE acceleration spectrum introduced in FEMA P695 (2009)

The scale factors represent the ratio of the spectral response acceleration (S_{aT}) of the input records at the fundamental period of the building archetype to the MCE spectral response acceleration for that fundamental period (S_{MT}). The fundamental period (T) of the 6-story building archetype has been calculated equal to 1.14Sec based on the formulation suggested in chapter 12 of ASCE/SEI 7-10 (ASCE 2010). In addition, the MCE spectral response acceleration for T = 1.14 Sec was obtained equal to 0.78 g (gravity acceleration) from the acceleration response spectrum suggested in FEMA P695 (FEMA-P695 2009) for this seismic intensity level. Fig. 12 shows the acceleration response spectra of the ground motion records implemented in this study in conjunction with the mentioned MCE acceleration spectrum.

Among different outputs of the nonlinear analyses, the main focus was placed on the interstory drift ratio time histories. This seismic demand has been mostly used to assess the seismic performance of buildings and it has even been related to the collapse limit state in previous studies (Vamvatsikos and Cornell 2002, FEMA-P695 2009, Lignos and Krawinkler 2012, Karamanci and Lignos 2014). Hence, the story drift time histories obtained from the numerical simulations were used to compare the seismic response of the nonlinear numerical models developed for the intended SMF. The drift ratio time histories of the fifth story of the intended frame obtained under the records number 1 and 5 at two levels of excitations have been shown in Fig. 13. As it is apparent in this figure, the time histories obtained from the simulations conducted on both Model1-FB-FLPH and Model2-FB were close as long as the intensity of the excitation is low ($\frac{S_{aT}}{S_{MT}} = 0.6$ in Fig. 13). For higher intensities ($\frac{S_{aT}}{S_{MT}} = 1.2$, and 1.5 in Fig. 13), the results of the simulations conducted on Model1-FB-FLPH deviated from the results of the simulations performed on Model1-FB. It is worth noting that the fiber-based FLPH method used to model the columns of Model1-FB-FLPH is capable of capturing the cyclic strength deterioration. Consequently, the difference between the time histories obtained for Model1-FB-FLPH and Model2-FB increased as the number of changes in the direction of story drift ratio cycles increased. Hence, the difference between the recorded time histories was not only affected by the intensity of the base excitations, but also by the intrinsic characteristics of the ground motion records chosen for conducting the simulations. The time histories obtained from the simulations conducted on Model3-ZLPH consisted of larger interstory drift ratios compared with the results of the simulations performed on the two other models. In Model3-ZLPH, the level of axial force in the columns was presumed equal to 20% of their yield capacity in order to evaluate the required modelling parameters based on the formulations suggested by Lignos and Krawinkler (2012). However, the level of axial force in the columns of the intended frame was not constant during the simulations, and these members might undergo such high levels of axial loading only for a few seconds. Furthermore, the abrupt drop of the strength

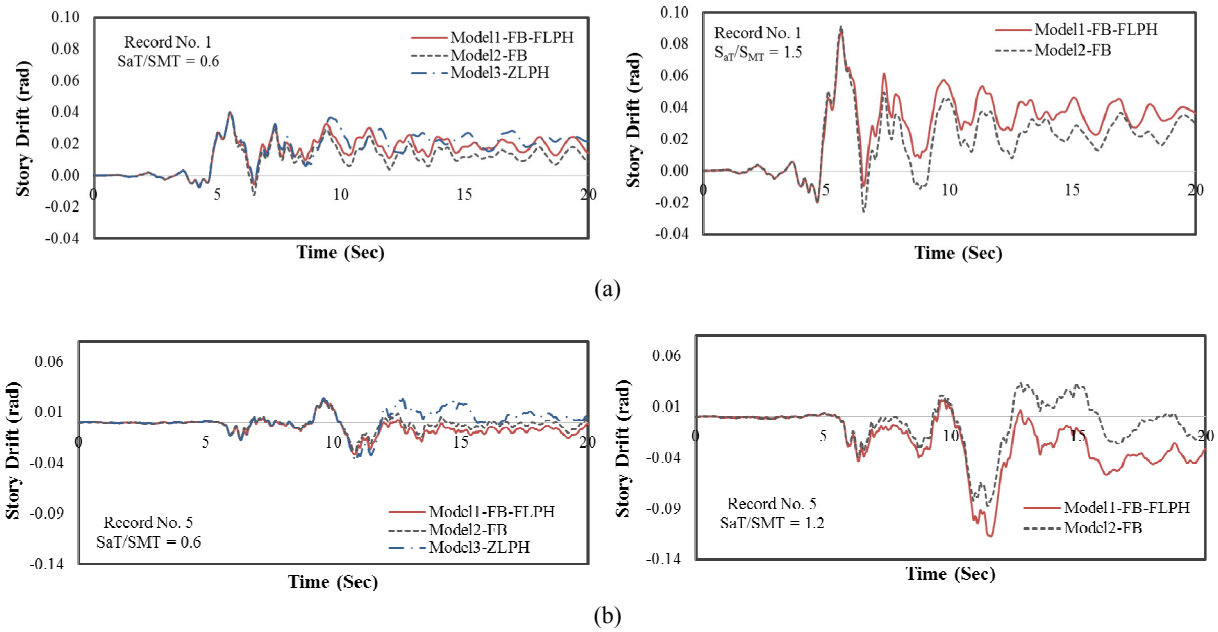

(a)

(b)

Fig. 13 Drift time histories of (a) the fifth story of the selected SMF under record no. 1 with different intensities; (b) the sixth story of the SMF archetype under record no. 5 with different intensities

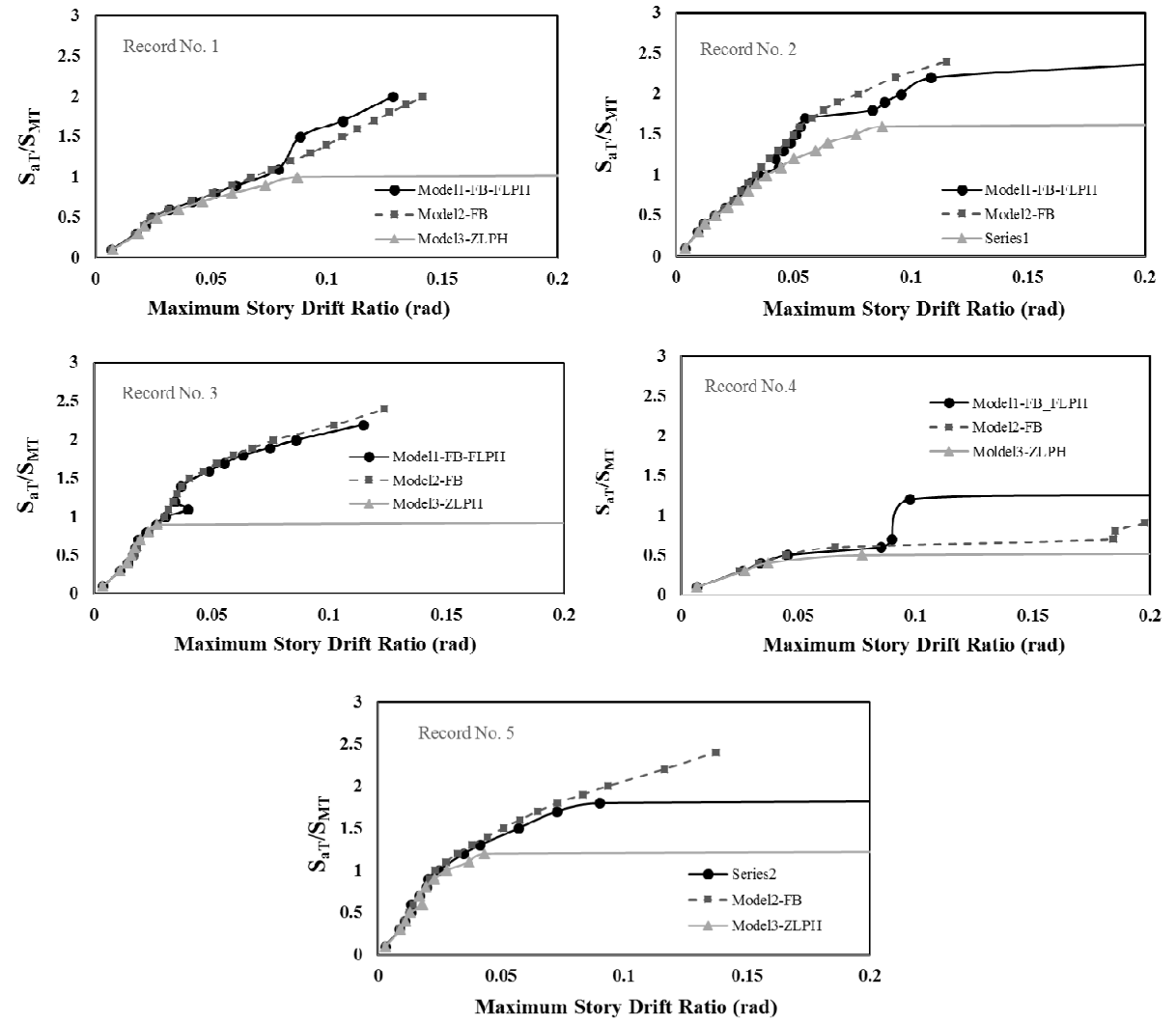

Fig. 11 Plan view of the sample 6-story building

could be another issue with the modelling technique used in Model3-ZLPH. In This modelling technique, it is assumed that the strength of the hinge drops to zero after the rotation in the hinge exceeds a specified ultimate rotation. Although values smaller than 0.1 rad were suggested for the ultimate rotation by Lignos and Krawinkler (2012), this modelling parameter was assumed equal to 0.1 rad to evade probable numerical instabilities. However, the results obtained from the analyses carried out on the third model were not reliable at high intensities due to numerical instabilities.

After performing the incremental dynamic analyses (IDA), the maximum of peak interstory drift ratios of the 6-story frame archetype at various levels of ground motion intensity have been presented in Fig. 14. Each curve (IDA curve) in each diagram represents the results of the analyses conducted under a specific record with various increasing intensities (using one of the three nonlinear models provided in this study). Each point of the curves in this figure is the result of one nonlinear dynamic analysis. That is, each point represents the maximum story drift ratio captured when one of the intended nonlinear frame models was subjected to a record with a specified intensity. As expected, for the elastic range and at initial low intensities, the curves representing the results obtained for the three frame models under the same records approximately coincided. However, these curves diverged by increasing the base excitation intensity. The difference between the curves representing the seismic behaviour of Model1-FB-FLPH and Model2-FB respectively was not significant for some records at some specific intensity. It should be noted that each point presented in Fig. 14 is the maximum story drift recorded during each nonlinear dynamic analysis. However, in some cases there was a severe peak in the time-history response of the intended frame models while any significant nonlinear deformation had not been captured before the mentioned peak (Fig. 13(a)). In these cases, the peak story drift was followed by smaller fluctuations around a residual story drift. Although this part of the time-history responses, after the recorded peak, was different for both mentioned models, the peak response (the maximum story drift ratio) was not obtained significantly different. Hence, for such cases, referring to IDA curves is a misleading way to show how the results of a nonlinear simulation can be affected by using different modelling techniques to represent the seismic behaviour of structural members.

Furthermore, it can be inferred from the IDA performed in this study that implementing the suggested fiber-based FLPH method to model the column members did not affect the numerical stability of the simulations. The simulations performed on Model1-FB-FLPH were even numerically as stable as the simulations conducted on Model2-FB in which a simple bilinear behaviour was assigned to the fiber elements. Hence, employing the fiber-based FLPH modelling technique with the details discussed in this paper make it possible to consider the strength deteriorations in the seismic behaviour of column members, while employing this model does not jeopardize the convergence of nonlinear numerical simulations. It is worth noting that restricting the material nonlinearity only to a limited length of column members in this modelling method reduces dramatically the computational cost of time-history analyses compared with the cases in which the entire length of columns is discretized to nonlinear fiber elements.

5. Conclusions

In order to simulate the behaviour of lateral load resisting frames under different seismic records, it is needed to employ robust and reliable discrete finite element models to simulate the seismic behaviour of individual structural members of these frames. Similar to other structural members, it is important to employ an appropriate model for columns that accounts for different aspects of the seismic behaviour of these structural members. Column members are subjected to simultaneous varying axial and bending moments during severe ground motions. In addition, the cyclic behaviour of these members can be deteriorated due to the local geometric instabilities. The deterioration in the hysteretic behaviour of these members cannot be neglected for the columns with hollow steel sections. In this study, the rate of this deterioration has been investigated for HSSs with seismically compact cross-sections, and an appropriate modelling technique has been employed and calibrated to simulate the cyclic and seismic response of these sections.

First, a benchmark database of the cyclic behaviour of hollow steel columns has been developed in this study with the aid of continuum finite element (CFE) simulations. This database consists of the cyclic response of several square HSSs under simultaneous axial and lateral loading with varying amplitudes. Next, the novel database has been employed to calibrate a fiber-based FLPH modelling technique. The fiber-based FLPH modelling technique introduced and calibrated in this study is capable of accounting for P-M interaction in columns. In addition, the deterioration in the cyclic behaviour of columns is implicitly taken into account by using the calibrated model for simulating the seismic and cyclic behaviour of columns. The appropriate values for the required modelling parameters were also obtained through a calibration procedure. Furthermore, a regression analysis was also performed to find an equation for predicting the calibrated values based on the geometry and the material properties of intended columns. The equation obtained from the regression analysis can be used for the columns fabricated from steel of types ASTM A500 Grade D and C, and with width to thickness ratios range from 17 to 30. Finally, the efficiency of the calibrated modelling technique in representing the seismic behaviour of the columns of a general structural frame has been examined. It has been shown that considering the cyclic deterioration as one of the important aspects of the seismic behaviour of columns results in capturing higher general seismic demands such as story drift ratios in a structural frame. It has also been proved that employing the mentioned model for columns does not jeopardize the stability of the numerical simulations.

References

ABAQUS (2012), Abaqus Analysis User's Guide; SIMULIA, Providence, RI, USA.

AISC (2010a), AISC 340-10: Seismic provisions for structural steel buildings; ANSI/AISC 341-10, Chicago, IL, USA.

AISC (2010b), AISC-360-10: Specification for structural steel buildings; Chicago, IL, USA.

ASCE (2010), ASCE/SEI 7-10: Minimum design loads for buildings and other structures; American Society of Civil Engineer31.

Chatterjee, S., Hadi, A.S. and Price, B. (2000), *Regression Analysis by Example*, Wiley, New York, NY, USA.

Cheng, X., Chen, Y. and Nethercot, D.A. (2013), "Experimental study on H-shaped steel beam-columns with large width-thickness ratios under cyclic bending about weak-axis", *Eng. Struct.*, **49**, 264-274.

Coleman, J. and Spacone, E. (2001), "Localization issues in force-based frame elements", *J. Struct. Eng.-Asce*, **127**(11), 1257-1265.

Dimopoulos, A.I., Tzimas, A.S., Karavasilis, T.L. and Vamvatsikos, D. (2016), "Probabilistic economic seismic loss estimation in steel buildings using post-tensioned moment-resisting frames and viscous dampers", *Earthq. Eng. Struct. Dyn.*, **45**(11), 1725-1741.

Farahi, M. and Erfani, S. (2016), "Developing representative dual loading protocols for the columns of steel special moment frames based on the seismic demands on these members", *J. Earthq. Eng.*, 1-22.

Farahi, M. and Mofid, M. (2013), "On the quantification of seismic performance factors of Chevron Knee Bracings, in steel structures", *Eng. Struct.*, **46**, 155-164.

FEMA-P695 (2009), Quantification of building seismic performance factors; Federal Emergency Management Agency, Washington, DC, USA.

Giberson, M. (1969), "Two nonlinear beams with definitions of ductility", *J. Struct. Div.*, **95**(2), 137-157.

Hall, J.F. and Challa, V.R.M. (1995), "Beam-column modeling", *J. Eng. Mech.*, **121**(12), 1284-1291.

Hamidia, M., Filiatrault, A. and Aref, A. (2014), "Simplified seismic sidesway collapse analysis of frame buildings", *Earthq. Eng. Struct. Dyn.*, **43**(3), 429-448.

Hsiao, P.-C., Lehman, D.E. and Roeder, C.W. (2013), "A model to simulate special concentrically braced frames beyond brace fracture", *Earthq. Eng. Struct. Dyn.*, **42**(2), 183-200.

Ibarra, L.F. and Krawinkler, H. (2005), *Global Collapse of Frame Structures under Seismic Excitations*, Department of Civil Engineering, Stanford University, John A. Blume Earthquake Engineering Center.

Ibarra, L.F., Medina, R.A. and Krawinkler, H. (2005), "Hysteretic models that incorporate strength and stiffness deterioration", *Earthq. Eng. Struct. Dyn.*, **34**(12), 1489-1511.

Imani, R., Mosqueda, G. and Bruneau, M. (2015), "Finite element simulation of concrete-filled double-skin tube columns subjected to postearthquake fires", *J. Struct. Eng.*, **141**(12), 04015055.

Jin, J. and El-Tawil, S. (2003), "Inelastic cyclic model for steel braces", *J. Eng. Mech.*, **129**(5), 548-557.

Karamanci, E. and Lignos, D.G. (2014), "Computational approach for collapse assessment of concentrically braced frames in seismic regions", *J. Struct. Eng.*, **140**(8), A4014019.

Kumar, S. and Usami, T. (1996), "Damage evaluation in steel box columns by cyclic loading rests", *J. Struct. Eng.*, **122**(6), 626-634.

Kurata, M., Nakashima, M. and Suita, K. (2005), "Effect of column base behaviour on the seismic response of steel moment frames", *J. Earthq. Eng.*, **9**(2), 415-438.

Lignos, D.G. and Krawinkler, H. (2011), "Deterioration modeling of steel components in support of collapse prediction of steel moment frames under earthquake loading", *J. Struct. Eng.*, **137**(11), 1291-1302.

Lignos, D. and Krawinkler, H. (2012), *Sidesway Collapse of Deteriorating Structural Systems under Seismic Excitation*, John A. Blume Earthquake Engineering Research Center, Department of Civil Engineering, Stanford University.

Menegotto, M. and Pinto, P.E. (1973), "Method of analysis for cyclically loaded reinforced concrete plane frames including changes in geometry and non-elastic behavior of elements under combined normal force and bending", *IABSE Symposium on Resistance and Ultimate Deformability of Structures Acted on by Well Defined Repeated Loads*.

Nakashima, M. and Liu, D. (2005), "Instability and complete failure of steel columns subjected to cyclic loading", *J. Eng. Mech.*, **131**(6), 559-567.

Nam, T.T. and Kasai, K. (2011), "Dynamic analysis of a full-scale four-story steel building experimented to collapse by strong ground motions", *Proceedings of the 8th International Conference on Urban Earthquake Engineering* (*8CUEE*), Center for Urban Earthquake Engineering (CUEE), Tokyo, Japan, March.

Newell, J.D. and Uang, C.-M. (2008), "Cyclic behavior of steel wide-flange columns subjected to large drift", *J. Struct. Eng.*, **134**(8), 1334-1342.

OpenSees (2015), Open System for Earthquake Engineering Simulation (OpenSees); Pacific Earthquake Engineering Research Center, University of California, Berkeley, CA, USA.

PEER/ATC (2010), Modelling and acceptance criteria for seismic design and analysis of tall buildings; Applied Technology Council (ATC).

Ribeiro, F.L.A., Barbosa, A.R., Scott, M.H. and Neves, L.C. (2015), "Deterioration modeling of steel moment resisting frames using finite-length plastic hinge force-based beam-column elements", *J. Struct. Eng.*, **141**(2), 04014112.

Salawdeh, S. and Goggins, J. (2013), "Numerical simulation for steel brace members incorporating a fatigue model", *Eng. Struct.*, **46**, 332-349.

Scott, M.H. (2011), *Numerical Integration Options for the Force-Based Beam-Column Element in Opensees*,

Scott, M.H. and Hamutçuoğlu, O.M. (2008), "Numerically consistent regularization of force-based frame elements", *Int. J. Numer. Method. Eng.*, **76**(10), 1612-1631.

Tzimas, A.S., Kamaris, G.S., Karavasilis, T.L. and Galasso, C. (2016), "Collapse risk and residual drift performance of steel buildings using post-tensioned MRFs and viscous dampers in near-fault regions", *Bull. Earthq. Eng.*, **14**(6), 1643-1662.

Uriz, P., Filippou, F.C. and Mahin, S.A. (2008), "Model for cyclic inelastic buckling of steel braces", *J. Struct. Eng.-Asce*, **134**(4), 619-628.

Vamvatsikos, D. and Cornell, C.A. (2002), "Incremental dynamic analysis", *Earthq. Eng. Struct. Dyn.*, **31**(3), 491-514.

CC